Published in final edited form as:
IEEE Robot Autom Mag. 2008 September 12; 15(3): 70–78. doi:10.1109/MRA.2008.927692.

Pulling Your Strings

JAMES S. SULZER, **MICHAEL A. PESHKIN**, and **JAMES L. PATTON**

Keywords

Rehabilitation; cable; moment arm; variable impedance; exotendon

Recently, there has been an exciting array of new robotic devices especially designed for human-machine interaction. Consequently, a new field related to haptics has flourished: development of simple and often inexpensive devices that provide force feedback or positioning of a human operator as controlled by customized computer programs. One method, which seems to be less explored, is the use of cable actuators for such a robot.

Cables are advantageous because of remote actuation, flexibility, and low weight. Tendons are examples of cables used in nature. The body uses these natural tension elements by keeping them close to the joints, which generates a small moment arm that limits torque but allows large and often rapid movement. For example, forearm muscles only contract 30% of their rest length but use tendons to span across the fingers, enhancing range of motion and dexterity while simultaneously reducing arm inertia. Studies of the joint configuration-based changes in muscle leverage have revealed the importance of both tension and moment arms in generating force, motion, and impedance [1]. In robotics, the Utah/MIT hand is a robotic analog to the human hand's use of cables [2]. This robot hand uses cables passing over pulleys, which for humans would be represented by tendon sheaths, for low-friction remote actuation.

Address for Correspondence: James S. Sulzer, Northwestern University, Department of Mechanical Engineering, Sensory Motor Performance Program, Rehabilitation Institute of Chicago, 345 E. Superior Suite 1406, Chicago, IL 60611. sulzer@northwestern.edu.

Cable-actuated mechanisms have been used by human beings in the past. The whole arm manipulator uses a novel, differential cable transmission system to reduce high cable tension, increase backdrivability, and reduce cable failure in an articulating arm [3]. The PHANTOM by SensAble uses a low backlash cable-driven transmission to create a multipurpose haptic interface [4]. A number of human-interactive experiments have used cables to successfully actuate human joints, either directly at the joint [5], through a parallel configuration [6], [7], or through series elastic elements [8].

The concept of series elastic actuation, first published by Pratt and Williamson, controls the equilibrium point of a linear spring in series with a gearmotor [9]. This creates a lightweight, low-cost, simple, and compliant interface fit for human applications. Veneman et al. take this concept a step further, using cables to remotely actuate the elastic joints on a lower body exoskeleton for gait rehabilitation [8]. They consider this device, known as LOwer-extremity Powered ExoSkeleton (LOPES), to be a more beneficial method of assisting gait because of its inherent compliance and lower apparent inertia than position-controlled robotic gait trainers such as the Lokomat [10].

Our key motivation is the rehabilitation of individuals recovering from stroke or other neurological insult. This area needs constant development because of an expanding aged population and improved rates of survival from injuries. Recent research strongly supports rehabilitation by prolonged practice of functional activities of the upper limb, even though professionally supervised therapy is quite limited by the current medical economic system. Although robotic therapy has been thought to be able to fill this gap, performance and cost have been a difficult optimization. Lower-cost, lighter-weight gearmotors lack the ability to provide the forgiving torque-controlled output that human therapists deliver. Although passive, compliant training devices are now becoming available for home rehabilitation [11], few, if any, active training devices exist that are inexpensive, compliant, safe, and capable of home use. In this article, we summarize research that introduces a novel modality of joint actuation based on previous work [12]–[14], one that can potentially lead to a low-cost, human-friendly home rehabilitation system. This method manipulates both the tension and the moment arm in a cable-driven joint to create a variable compliant interface.

The torque exerted by a cable-driven joint is the cross product of the line of action of the cable, known as the moment arm, and its tension. The subject of this article delves into this latter, less-studied quantity associated with torque. The concept of moment arm manipulation of a cable-driven joint is introduced, developed, formalized, and then examined with experiments on a physical, single-joint device. This method of moment arm manipulation, referred to as the moment arm manipulation for remote induction of net effective torque (MARIONET), is found to have distinct advantages that make it feasible for home rehabilitation as well as potential outside of the field.

Concept Development

The key to this investigation is how the moment arm is manipulated. Figure 1(a) is a schematic of a single cable-driven joint, with parameters given in polar coordinates. A fictional hand changes the line of action of the cable under constant tension, and the moment arm path can vary in an infinite number of ways. Ultimately, a single degree-of-freedom (DoF) path variation can be broken down into two archetypes: linear and rotational. Figure 1(b) provides four basic examples of path variation using these two archetypes, of which either may be centered at the joint or located some offset distance away. At any joint position, there exists a maximum and minimum torque (referred to as a torque envelope) that can be exerted on the joint, given the constraint of the moment arm path and constant tension. Figure 2 displays a normalized envelope resulting from a 1-m link length and a unit

cable tension showing how torque varies for different moment arm paths across joint positions. Because a linear path does not reflect the movement of the joint, its torque envelope will be nonlinear. As Figure 2(a) illustrates, a linear path through the joint center can produce the largest possible torque at a few certain joint positions, but it is incapable of producing torque in the opposite direction at those same points. Furthermore, the maximum attainable torque in this design varies with joint position. As a result of this behavior, the endpoint stiffness, which is the partial derivative of the torque according to joint position, is also highly nonlinear, reducing the system effectiveness for perturbations. In short, a linear moment arm path is not globally controllable, but it does have high torque capability.

One example of an application of a linear path is a leg rehabilitation robot by Homma et al. [5]. Traveler cars riding on rails 2 m above a prone subject pull on cables that directly manipulate the lower extremities. With such a large offset, the structure takes advantage of the high moment arm that can be achieved for the limited range of motion of the leg. Controllability is restored by using gravity to return the leg to its initial position.

The candidate rotational paths show a larger difference in comparison. Figure 2(b) shows that, while the offset rotational path also has a nonlinear relationship with joint position, the rotational path centered at the joint produces a constant torque envelope in both directions. Maximum torque increases with radius, and endpoint stiffness is locally positive, definite, smooth, and symmetric, making it robust to perturbations. These properties make this rotational path appropriate for the general application outlined in this article.

A schematic using this rotational moment arm path version of the MARIONET is shown in Figure 3. There are a few basic components in this system. The end effector rotates about a center with a cable connected to it at point (R_L, Θ). The cable then passes through a pulley on the rotator at point (R_P, Φ), which, as its name implies, can only rotate, creating the desired moment arm constraint. The length of cable from end effector to rotator is denoted as L_{LP}. The cable then travels from the pulley on the rotator to a motor at point (R_T, ζ), known as the tensioner, which supplies cable tension, and for the purpose of this article, it maintains a constant value. The length of cable from (R_P, Φ) to (R_T, ζ) is denoted as L_{PT}. The end effector and rotator have the same center of rotation. Although the end effector is left free to rotate, it is pulled along by the cable that passes through the rotator, whose position is rigidly controlled by the drive motor.

The energy, torque, and stiffness of the system are a function of the length of the cable and its tension. The system will settle at equilibrium, or in other words, its minimum potential energy, where the cable is at its minimum length. The work, W, that the system does on its environment may be expressed in terms of the tension, T, and the change in length of the cable, otherwise known as cable excursion, dx,

$$W = \int T dx. \quad (1)$$

The sum of the lengths of the cable is calculated as segments separated at the pulley:

$$dx = L_{PT}(\Phi) + L_{LP}(\Phi, \Theta) - l_0, \quad (2)$$

where l_0 is the length of the cable at minimum energy. Using the law of cosines to solve for the terms mentioned earlier,

$$L_{PT}(\Phi)^2 = R_P^2 + R_T^2 - 2R_P R_T \cos(\Phi - \zeta) \quad (3a)$$

and

$$L_{LP}(\Phi,\Theta)^2=R_L^2+R_P^2-2R_LR_P\cos(\Theta-\Phi). \quad (3b)$$

With a constant cable tension, the work is the product of the length of cable and tension and can be stated in terms of joint torque τ,

$$W=\int T\,dx=\int \tau\,d\Theta. \quad (4)$$

This equation can be simplified to

$$\frac{\tau}{T}=\frac{dx}{d\Theta}. \quad (5)$$

Therefore, the torque per unit tension (moment arm) is equivalent to the change in the amount of cable excursion according to the end effector position. In other words, a small amount of excursion that causes a large change in joint position, as does in the fingers, indicates a small moment arm. Carrying out the math,

$$\frac{\tau}{T}=R_L\frac{R_P}{L_{LP}(\Psi)}\sin(\Psi), \quad (6)$$

where $\Psi=\theta-\Phi$ is the relative angle between the rotator and the end effector. The endpoint stiffness, k, can be found in a similar manner, since

$$\frac{k}{T}=\frac{d\tau}{d\Theta}=\frac{d^2x}{d\Theta^2}, \quad (7)$$

which means that the amount the moment arm changes with joint position is the endpoint stiffness. This provides a basis for the configuration-dependent stiffness of human limbs. Carrying out the math,

$$\frac{k}{T}=R_L\frac{R_P}{L_{LP}(\Psi)}\cos(\Psi)-R_L^2\frac{R_P^2}{L_{LP}(\Psi)^3}\sin^2(\Psi). \quad (8)$$

If an elastic element is placed in series with the cable, as will be examined in the following example, the torque equation now becomes

$$\tau=R_LR_P\sin(\Psi)k_sL_{LP0}, \quad (9)$$

where k_s is the stiffness of the linear spring, and L_{LP0} is the controlled equilibrium position of the spring. Therefore, both torque and endpoint stiffness can be manipulated using the relative angle, Φ. Moreover, one can linearly modify torque and stiffness by varying the tension.

The general concept of the MARIONET is to vary moment arm along any path while in some way maintaining tension in the cable. Other paths may be desirable in specific applications, such as where workspace is limited or where specific torques are required. A practical application is the mechanically adjustable compliance and controllable equilibrium

position actuator (MACCEPA) design that uses a nonbackdrivable motor to control a rotational moment arm path and also controls the length of a linear spring between the end effector and the rotator using another nonbackdrivable motor [15]. This has been used to control both equilibrium position and stiffness to actuate gait in a bipedal robot [16].

Some of the differences between using a spring and using a constant tension are illustrated in Figure 4. The torque-deflection relationship varies with both tension and geometrical parameters. Producing constant cable tension (gray gradient) and linear spring cable tension (green gradient) results in different possible ranges of torques. Increasing pretension amplifies the torque-deflection relationship in both curves in Figure 4(a). At low pretension, the linear spring case needs more deflection than constant tension to reach higher torques, but this aspect could be useful for filtering out disturbances. An increase in the pretension for both cases makes a more responsive system. Differences between the two cases become more pronounced when changing the relationship between the rotator radius (R_P) and the end effector length (R_L), shown in Figure 4(b). A very small rotator compared with the end effector could not create a large moment arm, and therefore in both cases, very little torque can be produced. However, as the rotator radius approaches the end effector, the greatest possible moment arm occurs as the relative angle between them approaches zero. In the case of the linear spring, the greatest amount of torque is produced when there is the optimum combination of both spring deflection and moment arm. From the standpoint of achieving high torque production, these plots suggest that constant force impedance, achieved perhaps by a constant force spring, would be more advantageous than a linear spring in situations with small rotator excursion and vice versa. A final item to note is that that the torque-angle relationship in Figure 4(a) closely resembles the way the force-length characteristic of mammalian muscle [17] and how it acts to smoothly and stably generate torque over a range of angles.

In fact, knowing such stability characteristics of this nonlinear system is essential for human use. The system indeed has a concave energy surface, where the system settles to an equilibrium point of minimum potential energy (Figure 5). Assuming the system starts at rest, Figure 6 uses specific parameters to provide a more intuitive example of stability. A more generalized analysis of stability is detailed in another work [13]. The energy corresponds to the system's geometry, with the picture on Figure 5(a) showing the MARIONET at maximum energy state on the user's elbow (magenta), and minimum energy (cyan). These colors correspond to the potential energy surface to the bottom, where the magenta hills are the positions of highest energy, and the cyan valley is at the lowest. The maximum torque occurs at the highest slope of this plot, in this case, just inside the two peaks. This region represents the workspace of the MARIONET and comprises the region of convergence defined as the region where difference between the link angle and the pulley angle (Φ) converges to zero, therefore, an attractor region of stability. The shallow bowl shape of the surface comes from the small amount of energy stored in L_{PT}, the length of cable from the tensioner to the rotator pulley.

Proof of Concept

We designed and built a proof of concept to actuate the human elbow. This version of the MARIONET, shown in Figure 6, has been designed to exert a light amount of torque (5 N · m) on the elbow within its range of motion (135°). The rotator is driven remotely using a 200-W servomotor through a 10:1 roller chain transmission. This drive motor can control the rotator position to the nearest 0.016° (0.0003 rad) and exert a maximum continuous torque of 6 N · m. The rotator has two pulleys mounted concentrically near its outer diameter for cable routing. A steel aircraft cable, with a diameter of 1/32 in (0.79 mm), is tensioned by a second 200-W servo-motor, known as the tensioner, through a cable spool.

The spool is composed of three parts: the spool itself, a follower, and a post. The spool is a threaded cylinder to guide cable wrapping. The threads alone are not sufficient to make sure that the cable does not overlap or skip threads, so a follower with the same thread pitch moves up and down the spool, guiding the cable into the threads. The post keeps the follower in the same orientation as it guides the cable into and out of the spool. This type of cable guidance is common in fishing reels.

As the cable leaves the spool, it passes through a mounting composed of a set of pulleys. The mounting ensures that the cable leaves at a constant height and measures cable tension with the help of two strain gauges. The cable passes through another set of pulleys on the rotator and then forms a block and tackle with a third set of pulleys on the end effector (4:1 reduction).

The end effector, built with an adjustable handle, rotates about the same center as the rotator. The position of the end effector is measured by a conductive plastic potentiometer with a resolution of 0.03° (0.0005 rad).

Torque on the elbow is controlled by regulating the position of the rotator relative to the end effector. The drive motor is operated in torque mode, with a PID controlling for position. In addition to control of the moment arm by the drive, the tensioner controls torque operating in an open-loop torque mode. Data are sampled at 2 kHz using a real-time operating system (QNX RTOS 2.0).

There are a number of safety precautions taken. Two mechanical stops prevent the end effector from leaving the workspace of the elbow. An emergency stop switch is available to both the user and the operator. Software stops shut off the motors if they move too fast for a given duration. A chain guard prevents anyone from touching the roller chain during operation.

Performance

We evaluated the performance of the device based on its intended tasks. Given the application of rehabilitation and motor control experiments, we measured how quickly the MARIONET could exert accurate torque.

When the tensioner operates at slow speeds, friction develops between the poles of the motor, making torque measurement difficult. Instead, we substituted a mass for the motor and calculated the resulting torque from the given weight and relative position of end effector and rotator. This value was compared with an empirical value obtained from a load cell that kept the end effector fixed. The calculated torque matches with the experimentally determined torque (Figure 7). The sinusoidal relationship between relative angle and torque continued as increasing the tension proportionally increased the amplitude.

A torque step response test (Figure 8) showed how fast the actuator could exert a substantial torque under either high or low cable tension. To accomplish this, the rotator had to move as quickly as possible to a new appropriate position to step up to the desired torque. In the low cable tension case (70 N of tension through the block and tackle), the 5% rise time was 65 ms, much faster than human reactions in voluntary movement of about 150 ms [18]. In the high cable tension case (300 N), the rise time was 21 ms, much faster than human reflex of about 30 ms [18]. Consequently, the cable tension can be adjusted to a level appropriate to the requirements of the human motor task.

Although the system was capable of producing fast and accurate torque, robotic training, rehabilitation, and haptic applications often require state-dependent force fields. In a final

performance test, we created a linear torque field that depended on either position or velocity with a user-defined deadband. The MARIONETwas capable of rendering a linear force field within a given range of output torques before the drive motor saturated (Figure 9). Both stabilizing (guidance) and destabilizing (error augmentation) fields were rendered, indicating a wide range of modes of control that might be possible with appropriate software.

Human Pilot Study of Robotic Training

Two of the many possible training paradigms currently used in robotic teaching and rehabilitation are forces that guide the user toward a desired trajectory (guidance) compared with nonintuitive, yet promising, approach of pushing the user away from a desired trajectory (error augmentation). For this preliminary study, six healthy, institutional review board-approved subjects (four male) were separated into three groups that differed in the type of torques they received: error augmentation (two subjects), guidance (two subjects), and a control group that experienced no torques (two subjects). Both error-augmentation and guidance torques pushed the arm 3 (N · m)/rad of error. Each subject was asked to move his or her elbow to mimic a complex movement of a dot projected on a platform above the arm by a laser. This ideal movement lasted 3.2 s and ranged between 0.5 and 2.3 rad. The experimental setup is shown in Figure 10(a).

The results of this basic pilot show that the MARIONETwas capable of altering its user's trajectories. In the control group, the subjects' individual movements [Figure 10(b), blue] were similar to the desired trajectory [Figure 10(b), red], but the timing was different. In the guidance group [Figure 10(c)], users' trajectories were attracted to the desired trajectory, but in the error augmentation group [Figure 10(d)], the users' trajectories seem to be opposite to the desired trajectory. The data here demonstrate the MARIONET's effectiveness as a programmable experimental device for human training.

Discussion and Conclusions

While performing to expectations, the proof-of-concept MARIONET, like all robotic devices, is limited by the power of its actuators and its geometry. The concept allows both moment arm manipulation and tension control to produce torque and impedance at a joint. In addition, the moment arm path can be altered to fit the application's requirements. For instance, a linear path may be more advantageous than a rotational path. Weight and cost can be reduced by using a highly geared drive motor and further by implementing an elastic element in series with a highly geared tensioner or even completely substituting the tensioner for a passive element. When using an active tensioner, regardless of configuration, the variable control of stiffness and equilibrium position make the MARIONET act like a variable compliant series elastic actuator. As a result, it shares many of the same advantages such as low weight, low cost, and compliance. In addition, by adding remote actuation, inertia is further reduced, the effect being amplified as the number of joints increase. This concept is illustrated in detail in previous work [14].

The technology has great potential in several areas, but one growing area that should make positive use of MARIONET transmission is in neurorehabilitation training, in which a patient learns to move correctly with repetitive training that is facilitated by interactions with a robot. For example, the financial costs of recovery from injuries such as stroke are staggering, with a projected total of US$2 trillion over the next 45 years [19]. Although a sizeable fraction (9%) of that total comes from rehabilitation costs, additional cost comes from informal care such as assistance from a family member. The compliant and safe aspects of the MARIONET make it a strong candidate for home rehabilitation, which has been shown to be comparably effective in the therapy in the clinic [20]–[22]. Although

home rehabilitation is more stressful for caregivers [20], a tireless home robotic system could become a part of the standard of care.

Besides rehabilitation, the MARIONET concept has potential in any application where remote actuation and mechanical compliance is desired and a high torque rate of change is not required. Such a unique device that imitates the variable moment arms of muscle and tendons may be used in teleoperation, surgery, mobile robots, micromanipulation, or hazardous material handling. Whether the application is in orthoses or in bridges, the variable compliance, lightweight, and remote actuation characteristics of the MARIONET have a promising future.

References

1. Murray WM, Delp SL, Buchanan TS. Variation of muscle moment arms with elbow and forearm position. J Biomech. 1995; 28(5):513–526. [PubMed: 7775488]
2. Jacobsen, S.; Iversen, EK.; Knutti, DF.; Johnson, RT.; Biggers, KB. Design of the Utah/MIT dextrous hand. Proc. IEEE Int. Conf. Robotics and Automation (ICRA); San Francisco. 1986. p. 1520-1532.
3. Townsend W, Guertin J. Teleoperator slave-WAM design methodology. Ind Robot. 1999; 26(3): 167–177.
4. Massie, TH.; Salisbury, JK. The PHANTOM haptic interface: A device for probing virtual objects. Proc. ASME Winter Annu. Meeting, Symp. Haptic Interfaces Virtual Environment and Teleoperator Systems; Chicago, IL. 1994. p. 295-301.
5. Homma, K.; Fukuda, O.; Nagata, Y.; Usuba, M. Study of a wire-driven leg rehabilitation system. Proc. Int. Conf. Intelligent Robots and Systems; Sendai, Japan. 2004. p. 1451-1456.
6. Surdilovic, D.; Bernhardt, R.; Schmidt, T.; Zhang, J. STRING-MAN: A new wire robotic system for gait rehabilitation. Proc. 8th Int. Conf. Rehabiliation Robotics; Korea. 2003. p. 64-66.
7. Mayhew, D.; Bachrach, B.; Rymer, WZ.; Beer, RF. Development of the MACARM—A novel cable robot for upper limb neurorehabilitation. Proc. IEEE 9th Int. Conf. Rehabilitation Robotics; Chicago, IL. 2005. p. 299-302.
8. Veneman, J.; Ekkelenkamp, R.; Kruidhof, R.; van der Helm, FCT.; van der Kooij, H. Design of a series elastic and bowden cable-based actuation system for use as torque-actuator in exoskeleton-type training. Proc. Int. Conf. Rehabilitation Robotics (ICORR); Chicago, IL. 2005. p. 496-499.
9. Pratt, GA.; Williamson, MM. Series elastic actuators; Proc Int Conf Intelligent Robots and Systems (IROS); 1995. p. 399-406.
10. Colombo G, Joerg M, Schreier R, Dietz V. Treadmill training of paraplegic patients using a robotic orthosis. J Rehabil Res Dev. 2000; 37(6):693–700. [PubMed: 11321005]
11. Reinkensmeyer DJ, Housman SJ. If I can’t do it once, why do it a hundred times?”: Connecting volition to movement success in a virtual environment motivates people to exercise the arm after stroke. Virt Rehabil. 2007:44–48.
12. Sulzer, JS.; Peshkin, MA.; Patton, JL. MARIONET: An exotendon-driven series elastic actuator for exerting joint torque. Proc. Int. Conf. Rehabilitation Robotics (ICORR); Chicago, IL. 2005. p. 103-108.
13. Sulzer, JS.; Peshkin, MA.; Patton, JL. Catastrophe and stability analysis of a cable-driven joint. Proc. IEEE Int. Conf. Engineering Medicine and Biology Society; New York. 2006. p. 2429-2433.
14. Sulzer, JS.; Peshkin, MA.; Patton, JL. Design of a mobile, inexpensive device for upper extremity rehabilitation at home. Proc. Int. Conf. Rehabilitation Robotics (ICORR); Noordwijk, Netherlands. 2007. p. 933-937.
15. Van Ham, R.; Van Damme, M.; Vanderborght, B.; Verrelst, B.; Lefeber, D. MACCEPA: The mechanically adjustable compliance and controllable equilibrium position actuator. Proc. 9th Int. Conf. Climbing and Walking Robots; Belgium. 2006. p. 196-203.
16. Van Ham R, Vanderborght B, Van Damme M, Verrelst B, Lefeber D. MACCEPA, the mechanically adjustable compliance and controllable equilibrium position actuator: Design and implementation in a biped robot. Robot Autonom Syst. 2007; 55(10):761–768.

17. Gordon AF, Huxley AF, Julian FJ. Variation in isometric tension with sarcomere length in vertebrate muscle fibers. J Physiol. 1966; 184(1):170–192. [PubMed: 5921536]
18. Winter, DA. Biomechanics and Motor Control of Human Movement. Hoboken, NJ: Wiley; 1990.
19. Brown DL, Boden-Albala B, Langa KM, Lisabeth LD, Fair M, Smith MA, Sacco RL, Morgenstern LB. Projected costs of ischemic stroke in the United States. Neurology. 2006; 67(8):1390–1395. [PubMed: 16914694]
20. Anderson C, Rubenach S, Mhurchu CN, Clark M, Spencer C, Winsor A. Home or hospital for stroke rehabilitation? Results of a randomized controlled trial. I. Health outcomes at 6 months. Stroke. 2000; 31(5):1024–1031. [PubMed: 10797161]
21. Widén Holmqvist L, von Koch L, Kostulas V, Holm M, Widsell G, Tegler H, Johansson K, Almazán J, de Pedro-Cuesta J. A randomized controlled trial of rehabilitation at home after stroke in southwest Stockholm. Stroke. 1998; 29(3):591–597. [PubMed: 9506598]
22. Anderson C, Rubenach S, Mhurchu CN, Clark M, Spencer C, Winsor A. Home or hospital for stroke rehabilitation? Results of a randomized controlled trial. II. Cost minimization analysis at 6 months. Stroke. 2000; 31(5):1032–1037. [PubMed: 10797162]

Biographies

James S. Sulzer received his B.S. degree from Ohio State University in 2002 and his M.S. degree from Northwestern University in 2006, both in mechanical engineering. He is currently a Ph.D. candidate at Northwestern and the Rehabilitation Institute of Chicago. His current research involves developing robotic mechanisms for understanding gait in stroke.

Michael A. Peshkin received his Ph.D. degree from Carnegie Mellon University, Pittsburgh, Pennsylvania, in 1988. He is a professor of mechanical engineering at Northwestern University, Evanston, Illinois. He is an inventor of cobots (collaborative robots, with J. Edward Colgate) and has been working in human-interactive aspects of robotics for many years. He is the founder of three companies: Mako Surgical (image-guided surgery), Cobotics (materials handling), and Kinea Design (rehabilitation robotics). His other research interests include exercise robotics, haptic communication between people, and electromagnetic sensors.

James L. Patton received B.S. degrees in mechanical engineering and engineering science/bioengineering from the University of Michigan at Ann Arbor in 1989, an M.S. degree in theoretical mechanics from Michigan State University at Lansing in 1993, and the Ph.D. degree in biomedical engineering from Northwestern University at Evanston in 1988. Currently, he is the associate director of the Center for Rehabilitation Robotics at the Rehabilitation Institute of Chicago (RIC) and an associate professor of bioengineering at the University of Illinois at Chicago. His work has focused on haptics, modeling the human–machine interface, robotic teaching, and robotic facilitation of recovery from a brain injury. He is a member of the IEEE Robotics and Automation Society (RAS) and the IEEE Engineering in Medicine and Biology Society (EMBS). He is a reviewer for *IEEE Transactions on Biomedical Engineering*, *IEEE Engineering in Medicine Biology Magazine*, and *IEEE Transactions on Robotics and Automation*. He also chairs the EMBS Technical Committee on Biomedical Robotics.

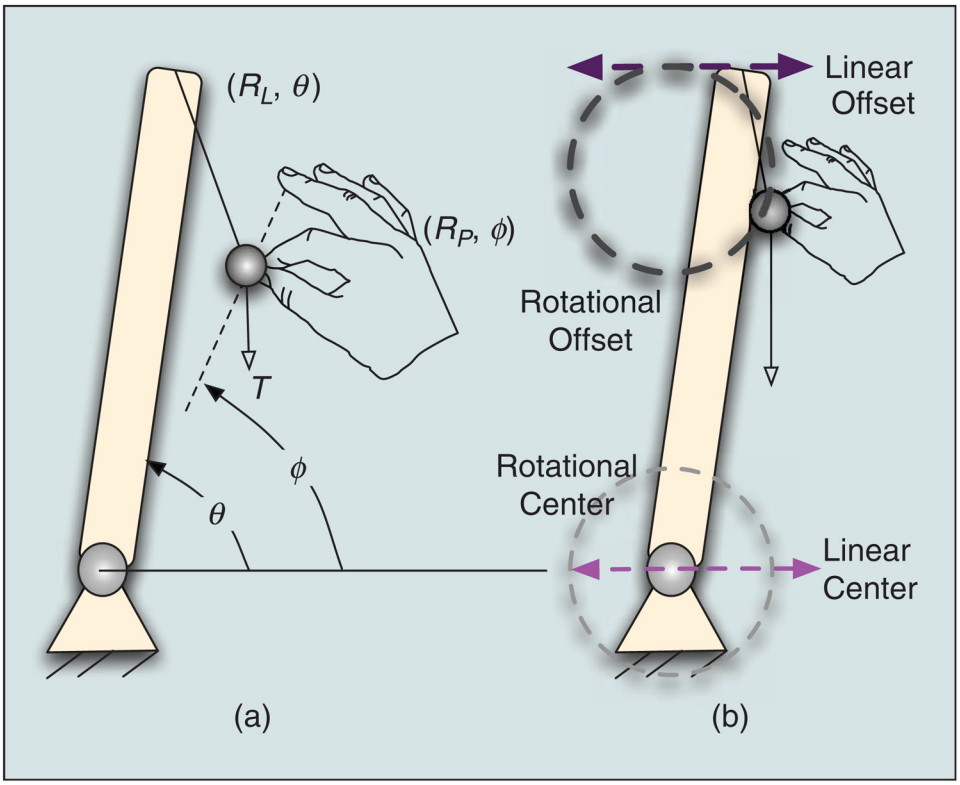

Figure 1.
(a) Fictional hand can move the cable's line of action in any manner. Variable definitions are given for this simple cable-driven joint in polar coordinates. (b) Four different candidate moment arm paths are shown for subsequent analysis.

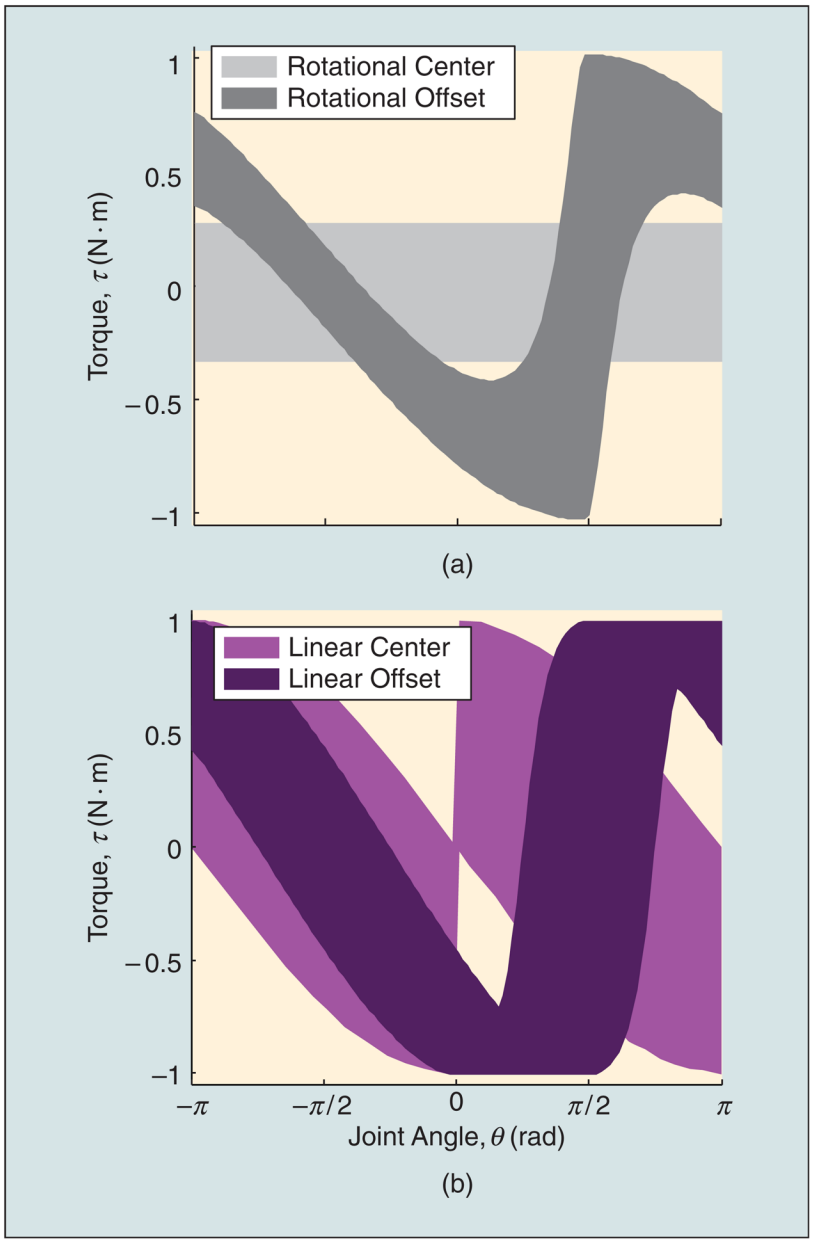

Figure 2.
Shaded areas display the range of achievable torques (torque envelopes) at each joint angle. (a) Rotational path. (b) Linear path. Since the rotational center path is constant and easily controllable, it was chosen for our initial implementation of the MARIONET.

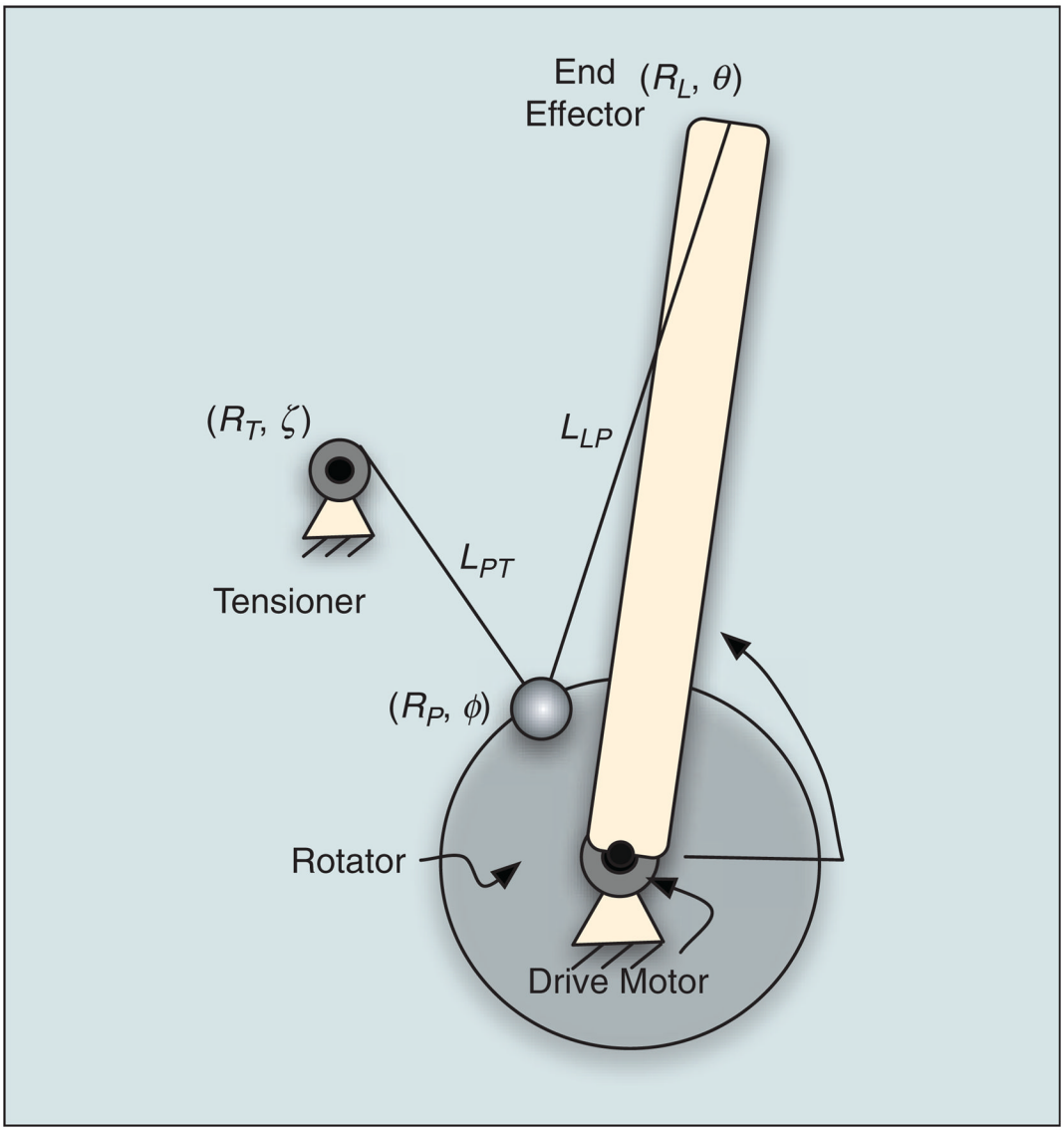

Figure 3.
Schematic and definitions of variables used throughout the analysis. The drive motor rigidly controls the position of the rotator and the tensioner creates cable tension, which couples the free-rotating end effector to the motion of the rotator. Both have the same center of rotation. All angles are measured relative to the horizontal datum, and all coordinates are in polar notation.

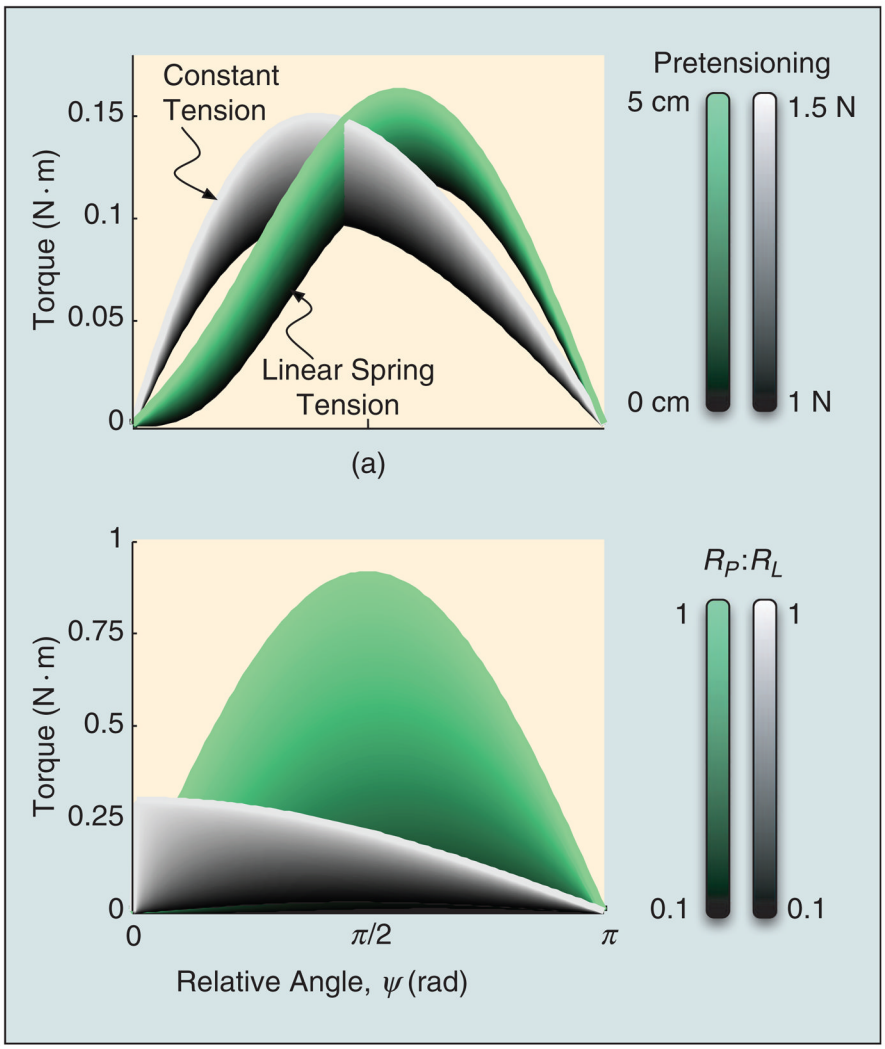

Figure 4.

The effect of (a) tension and (b) geometry are presented for two cases: one with constant tension on the cable (gray) and one with a linear spring inducing tension (green). Color bars on the right represent cable pretension in (a), and in (b), the ratio of rotator radius (R_P) to end effector length (R_L). Spring stiffness used was 10 N/m, and in (a), R_L and R_P were 0.3 and 0.1 m, respectively. Both figures show that higher torques can be reached with less rotator movement with constant tension, but linear spring tension can be useful for damping out disturbances.

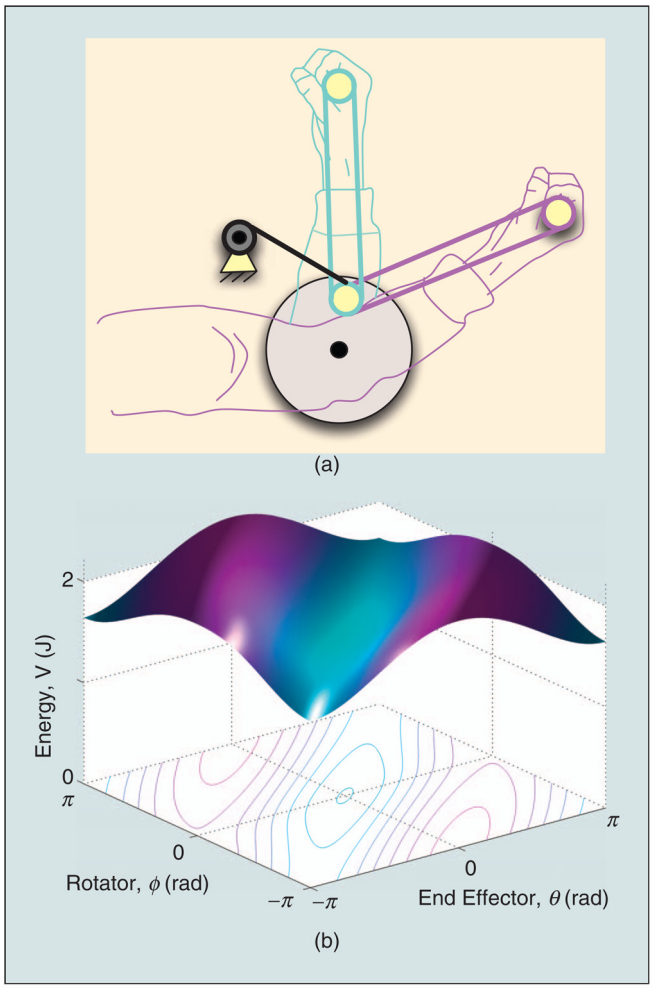

Figure 5.
As the rotator is aligned with the (a) arm (cyan), this corresponds to the minimum on the (b) energy surface below (cyan). As the moment arm increases (magenta), the energy reaches a maximum. In this case, the rotator is not fixed, and the slight bowl shape comes from the force of the tensioner, and the block and tackle between the hand and the rotator (4:1 reduction), as used in the proof-of-concept. The parameters used in this specific example are also taken from the proof-of-concept, R_L = 0.43 m, R_P = 0.07 m, and R_T = 0.15 m.

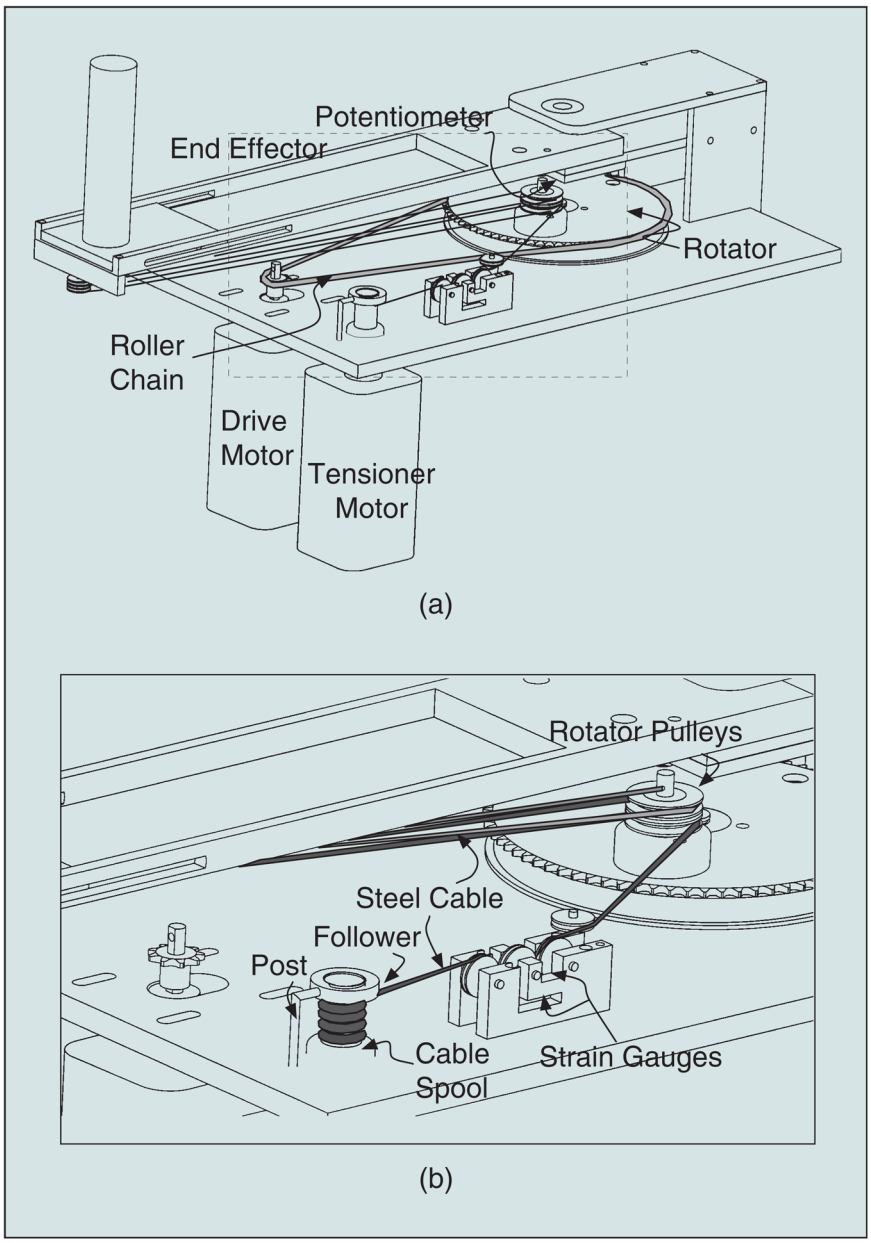

Figure 6.
(a) Proof-of-concept drawing shows the basic elements of the MARIONET. (b) A detailed view of the cable routing and tension measurement system. Note that the cable between the rotator and end effector is organized in a block and tackle.

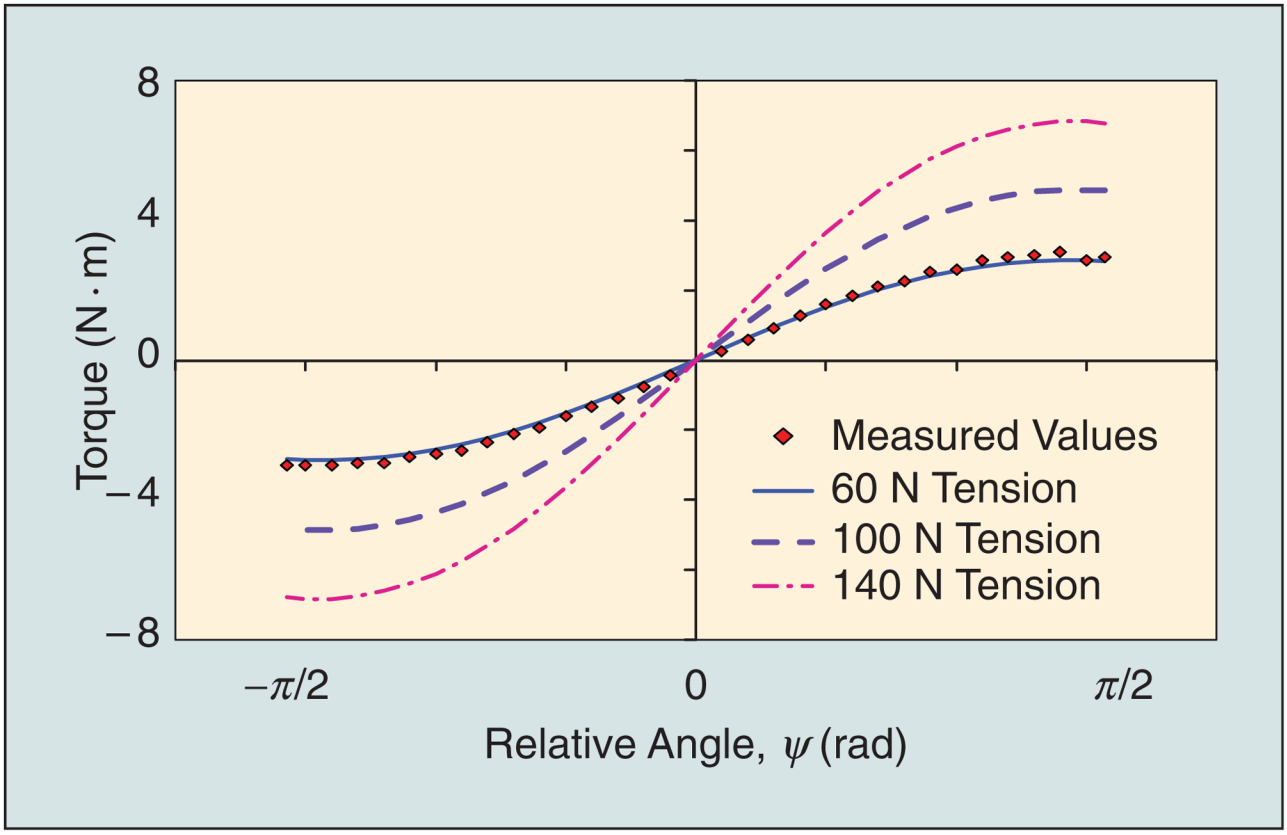

Figure 7.
Mathematical analysis accurately predicts torque of MARIONET. Because of high friction at low speeds of the tensioner, we used a hanging mass to supply constant torque.

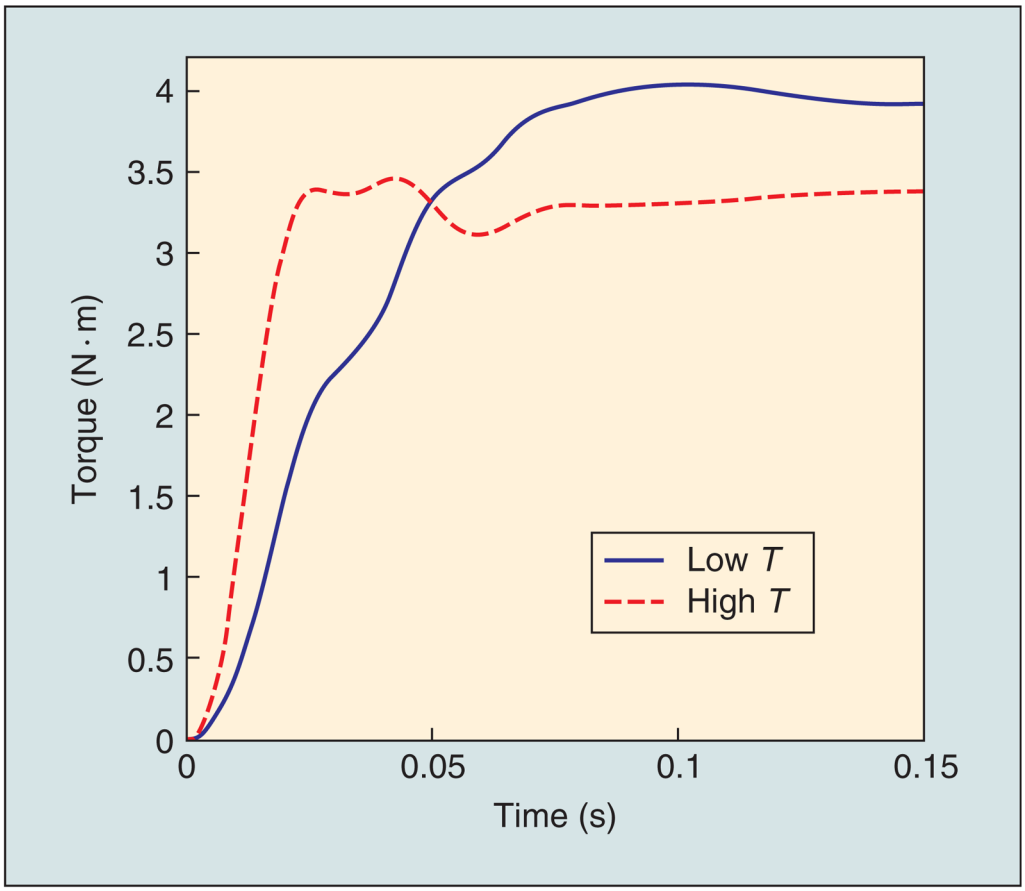

Figure 8.
Step responses at low (70 N) and high (300 N) tensions show quick response times.

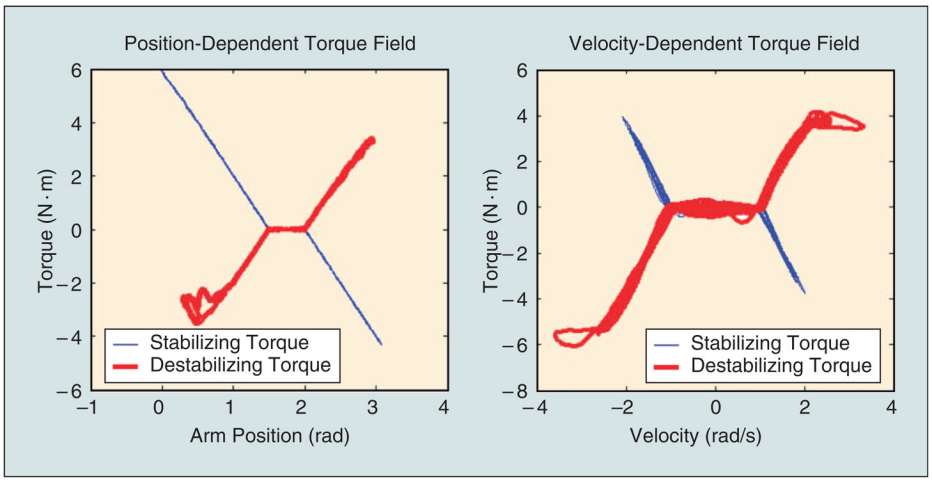

Figure 9.
The MARIONET is capable of producing torque fields of any shape. This case shows position and velocity-dependent linear torque fields for both stabilizing and destabilizing modes limited by motor saturation.

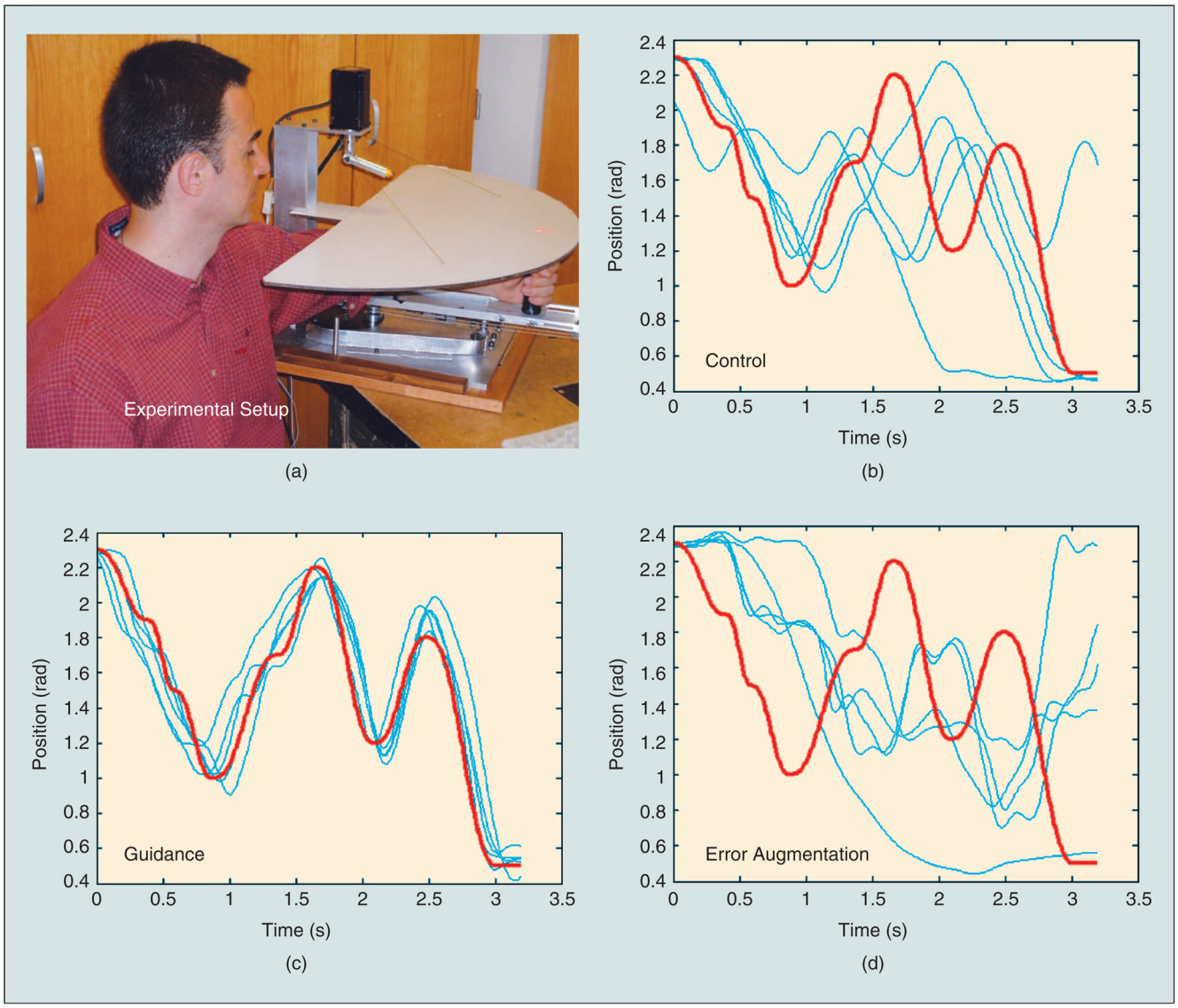

Figure 10.

(a) Experimental setup showing user following laser-dictated trajectory with MARIONET. (b)–(d) The desired trajectory (red) and the individual trials (blue) indicate that the single-DoF MARIONET is capable of producing error augmentation and guidance force fields. The control subject experiences the difficulty of mimicking a trajectory with no force feedback. The guidance subject has a much easier time, allowing the robot to push him toward the desired trajectory, while the error-augmentation subject has a difficult time mimicking the trajectory, often being pushed to opposite ends of the workspace.